Received: 4 November 2020 | Accepted: 15 November 2020

DOI: 10.1111/ina.12773

ORIGINAL ARTICLE

WILEY

Particle number emission rates of aerosol sources in 40 German households and their contributions to ultrafine and fine particle exposure

Jiangyue Zhao[1] | Wolfram Birmili[2] | Tareq Hussein[3,4] | Birgit Wehner[1] | Alfred Wiedensohler[1]

[1]Leibniz Institute for Tropospheric Research, Leipzig, Germany

[2]German Environment Agency (UBA), Berlin, Germany

[3]University of Jordan, Amman, Jordan

[4]Institute for Atmospheric and Earth System Research (INAR/Physics), University of Helsinki, Helsinki, Finland

Correspondence
Alfred Wiedensohler, Leibniz Institute for Tropospheric Research, Leipzig, Germany.
Email: ali@tropos.de

Funding information
Federal Ministry for the Environment, Nature Conservation, Building and Nuclear Safety (BMUB), Grant/Award Number: UFOPLAN FKZ 3715 61 200

Abstract

More representative data on source-specific particle number emission rates and associated exposure in European households are needed. In this study, indoor and outdoor particle number size distributions (10–800 nm) were measured in 40 German households under real-use conditions in over 500 days. Particle number emission rates were derived for around 800 reported indoor source events. The highest emission rate was caused by burning candles (5.3×10^{13} h^{-1}). Data were analyzed by the single-parameter approach (SPA) and the indoor aerosol dynamics model approach (IAM). Due to the consideration of particle deposition, coagulation, and time-dependent ventilation rates, the emission rates of the IAM approach were about twice as high as those of the SPA. Correction factors are proposed to convert the emission rates obtained from the SPA approach into more realistic values. Overall, indoor sources contributed ~ 56% of the daily-integrated particle number exposure in households under study. Burning candles and opening the window leads to seasonal differences in the contributions of indoor sources to residential exposure (70% and 40% in the cold and warm season, respectively). Application of the IAM approach allowed to attribute the contributions of outdoor particles to the penetration through building shell and entry through open windows (26% and 15%, respectively).

KEYWORDS

coagulation loss, correction factors of emission rates, indoor air model (IAM) simulation, particle number emission rate, penetration factor, source contribution to particle exposure

1 | INTRODUCTION

Exposure to airborne particles, especially submicrometer particles, has been reported to be associated with adverse health effects, notably respiratory and cardiovascular disease.[1–6] Despite notable decreases in outdoor pollution over the past decades in wide parts of developed countries, ambient particulate matter pollution, household air pollution from solid fuels and smoking remain among the top ten global risk factors for deaths and disability-adjusted life-years.[7]

In modern society, indoor air quality has become an increasing concern as people spend around 65% of their time in the residential environment.[8,9] Indoor air quality contributes significantly to personal exposure. However, the complexity of the processes that

take place indoors makes it difficult to draw conclusions about the general significance of various factors or processes.[9] Moreover, residential indoor air quality is seldom subject to official regulations. For a better understanding of indoor air quality, further studies on indoor particle exposure, in particular ultrafine particles, are needed.[11–14]

Aerosol particles in indoor air are usually a mixture of particles originating from indoor and outdoor various sources, where particle size distribution and chemical composition change over time. This change is dominated by several processes and factors such as the emission profile of indoor sources, the building shell penetration factor, the ventilation rate, and particle losses due to deposition on surfaces and coagulation. For fine (diameter < 1 μm) and ultrafine (diameter < 100 nm) particles, the particle number size distribution (PNSD) and total particle number concentration (PNC) are often better parameters than the mass concentration to describe the dynamic changes of indoor particles.[11,15,16]

In the interest of epidemiological research as well as preventive health care, it is important to identify indoor sources, quantify their strength and contribution, and subsequently mitigate their impact on personal exposure. BTEX (benzene, toluene, ethylbenzene and xylene) and PAH (polycyclic aromatic hydrocarbon) have been found in indoor combustion activities (such as burning candles, incense and mosquito repellents, and opening fireplaces), cooking, using 3D printers, and smoking, which can act as precursors of secondary particles in the indoor environment through the process of gas-to-particle conversion.[17–24] Moreover, these activities can dramatically increase the indoor PNC, especially of ultrafine particles.[20,21,25–33] In the literature, particle number emission rates of specific sources have often been determined with the aid of test chambers or test rooms under controlled conditions.[34–41] Burned candles and cooking activities are identified as the most important contributors to PNC. Conversely, only a few studies[16,42–47] have quantified the particle emission of residential indoor sources under real-use conditions. To our knowledge, only three of the mentioned studies have conducted such measurements in multiple residences: He et al[43] estimated emission rates for 153 indoor sources in 14 occupied houses in Brisbane, with results varying from 1.2×10^{13} h^{-1} to 2.4×10^{14} h^{-1}; Bhangar et al[16] quantified the emission rate of using gas cooking for 5.8×10^{11} h^{-1} and 1.6×10^{12} h^{-1} in two Californian homes; and Isaxon et al[47] studied 22 homes in Sweden, with emission rates of 39 source events ranging between 9.6×10^{13} h^{-1} and 2.7×10^{14} h^{-1}. There is a severe lack of knowledge on indoor particle number emission rates for European households. The limited number of data and the wide span of emission rates occurring in the literature emphasize the need for more representative data.[48,49]

For estimating the emission rates, a single-parameter approach[16,43,45–47] and an aerosol model approach[42,44,50] have been the two commonly used methods. Both approaches evaluate the material balance of indoor PNC, which is driven by aerosol dynamic processes. The existence of literature results derived from different methods calls for comparison, and a possibility to re-appraise these results. To our knowledge, no study has quantitatively compared the emission rates estimated from these two approaches.

Practical Implications

- This study provides data on source-specific particle emission rates and their resulting exposure in multiple dwellings under real-world conditions.
- Two commonly used approaches to estimate particle emission rates were compared quantitatively, which allows for a better understanding of previously reported results. The correction factor presented can be applied to houses under similar conditions for better use of the emission data in future health assessments.

In this work, we determined particle number emission rates for a variety of sources based on experimental data collected during two years in 40 German homes under real-use conditions.[51] From time-resolved PNSD, we extracted and analyzed, with the support of an activity log, around one thousand source emission events. To better interpret the emission rate calculated by different methods, two approaches were applied to quantify the emission rates of these source events. The first approach ignores certain particle dynamical processes, while the second approach uses an aerosol dynamics model, which is expected to greatly improve the estimates of particle number emission factors.

2 | MATERIAL AND METHOD

2.1 | Indoor/outdoor measurements

A suite of aerosol particle-related parameters was collected during two years in 40 occupied; non-smoking residential homes in Leipzig and Berlin, Germany (see Table 1). The 40 homes covered a range of building types from single apartments to multi-family houses, and areas of different population density. As typical for Germany, most homes were equipped with energy-saving, airtight windows, and used natural ventilation. Only three houses were equipped with a mechanical ventilation system and an air heat pump (see Table S1 in the Supporting Information). In general, mechanical systems and air conditioners are very rare in German homes due to meteorological conditions and cultural preferences. The dwellings, the two-year measurement program, and the instrumentation are described in much detail in a previous report.[51]

Briefly, two measurement systems were deployed to measure particle parameters indoors and outdoors simultaneously. Each system comprised a TROPOS-type mobility particle size spectrometer (MPSS) (designed as described in the study by Wiedensohler et al,[52] details see the Supporting Information) to determine the PNSD across the diameter range of 10–800 nm, and (total) PNC. The indoor system was placed in the living room,

TABLE 1 Characteristics of the households under study: Leipzig (L1–L20) and Berlin (B1–B20)

Homes	Type of area	Type of residence	No. of inhabitants	Measurement period (days)	No. of activities recorded	A/V[a] (m^{-1})	u[b] (m s^{-1})
L1	Rural	Detached house	2	9	41	0.19	1.5
L2	Rural	Detached house	4-7	25	84	0.13	1.5
L3	Rural	Detached house	4	12	49	0.11	1.4
L4	Rural	Detached house	3	11	25	0.09	1.6
L5	Rural	Detached house	2	9	17	0.10	1.7
L6	Rural	Detached house	2	11	25	0.15	1.5
L7	Rural	Detached house	2	7	6	0.11	1.6
L8	Rural	Detached house	3	11	14	0.13	1.5
L9	Suburban	Detached house	1	10	9	0.11	1.5
L10	Suburban	Detached house	4	10	19	0.02	2.0
L11	Urban	Detached house	3	18	24	0.11	1.7
L12	Suburban	Apartment	2	10	36	0.15	1.7
L13	Urban	Apartment	5	13	37	0.08	1.9
L14	Urban	Apartment	4	7	43	0.20	1.2
L15	Urban	Apartment	1	9	12	0.13	1.2
L16	Suburban	Apartment	2	3	34	0.10	1.6
L17	Suburban	Apartment	1	11	12	0.08	1.7
L18	Urban	Apartment	1	10	19	0.07	1.9
L19	Suburban	Apartment	3	10	20	0.12	1.7
L20	Urban	Apartment	3	8	15	0.15	1.7
B1	Rural	Detached house	1	14	22	0.14	1.6
B2	Rural	Detached house	6	14	50	0.14	1.5
B3	Rural	Detached house	3	14	45	0.14	1.6
B4	Rural	Detached house	2	14	23	0.15	1.7
B5	Rural	Detached house	2	14	4	0.07	1.6
B6	Rural	Detached house	3	14	57	0.08	1.6
B7	Suburban	Detached house	6	13	22	0.11	1.7
B8	Suburban	Detached house	2	14	12	0.13	1.5
B9	Suburban	Detached house	4	23	35	0.09	1.3
B10	Suburban	Detached house	2	14	55	0.10	1.6
B11	Suburban	Detached house	4	14	30	0.10	1.5
B12	Urban	Detached house	2	14	26	0.12	1.6
B13	Suburban	Apartment	5	14	26	0.13	1.3
B14	Suburban	Apartment	2	14	43	0.14	1.4
B15	Urban	Apartment	4	14	34	0.09	1.7
B16	Urban	Apartment	4	14	14	0.08	1.4
B17	Rural	Apartment	2	12	28	0.09	1.4
B18	Urban	Apartment	3	14	27	0.10	1.3
B19	Urban	Apartment	1	14	18	0.11	1.3
B20	Urban	Apartment	4	14	18	0.10	1.4

[a]A/V: the surface-area-to-volume ratio of the measurement room.

[b]u: best-fit near-surface friction velocity.

while the outdoor system was located either on a balcony or in the garden. The instrumental time resolution of 5 min allows us to identify even short-lived and transient phenomena related to particle emission and dispersion. Each home was visited twice for sampling periods of approximately one week each and in different seasons of the year.

Great care was taken to ensure a high quality of the measurement data. Instrument calibration and quality assurance were described in detail in our previous studies.[51,53] Both MPSS instruments used identical hardware (see Wiedensohler et al[52] and Zhao et al[53]) and were frequently checked under laboratory conditions against reference instrumentation in the World Calibration Center for Aerosol Physics (WCCAP).[54] This ensures a measurement uncertainty of ±10% or less for PNC. Indoor CO_2 concentrations were measured by a CO_2 sensor (GMP252 Vaisala) with a one-minute time resolution to estimate ventilation rates. To identify the type of active sources, inhabitants were requested to log their activities in a tablet computer using a custom-designed program.

2.2 | Determining particle emission rates

The main goal of this study is the determination of the particle number emission rates of indoor sources that are typically present in German residential homes. Particle emission rates will be useful to predict exposure to fine and ultrafine particles for various different building properties and ventilation regimes.

Assuming well-mixed air inside a room, the indoor particle dynamics were often described by material balance equations[16,55,56] Accordingly, the change of an indoor PNC (I) with time (t) can be described by

$$\frac{dI}{dt} = \frac{E}{V} + P\lambda O - (\lambda + \lambda_d) I - J_{\text{coagulation}} \quad (1)$$

with E being the source emission rate (h^{-1}), V the volume of the room, P the building penetration factor, λ the ventilation rate (h^{-1}), O the outdoor PNC, λ_d the deposition rate (h^{-1}) on indoor surfaces, and $J_{\text{coagulation}}$ the coagulation loss term. In indoor environments, the main mechanisms causing the decay of PNC are coagulation and particle deposition on indoor surfaces[57–59]; therefore, the effects of other mechanisms such as nucleation, condensation, and evaporation are not considered here.

There are two numerical approaches to solve Equation (1) for the unknown parameters P, λ_d, $J_{\text{coagulation}}$, and E. The assumptions and calculation structures are summarized as follows.

2.2.1 | Single-parameter approach (SPA)

The single-parameter approach (SPA) allows for rapid screening of experimental time series from different homes. In this approach, P, λ, and λ_d are considered constant for a room under study. To simplify calculations, particle resuspension and coagulation are assumed to be neglectable.

During steady-state, the indoor PNC change rate is close to zero (ie $dI/dt \approx 0$). When no indoor source is active (ie, $E/V = 0$), Equation (1) can be solved for P as follows:

$$P = \frac{(\lambda + \lambda_d)}{\lambda} \frac{I}{O} \quad (2)$$

All observed decay in PNC is ascribed to the particle decay rate ($\lambda + \lambda_d$), which is quantified as the negative slope in the logarithm of indoor PNC as a function of time:

$$\lambda + \lambda_d = \frac{1}{t_2 - t_1} \ln \frac{I_{t1}}{I_{t2}} \quad (3)$$

where t_2–t_1 is the period right after a strong indoor source, I_{t1} and I_{t2} are the corresponding indoor PNC at that time. The ventilation rate λ was calculated on the basis of experimental CO_2 data using the decay method.[60] This method considers CO_2 exhaled by residents as the source, λ only be derived for periods when the occupants have left the apartment/building, or when the windows are opened (details see the Supporting Information).

As discussed in our earlier study,[51] the SPA approach provides estimates for P, λ, and ($\lambda + \lambda_d$) typical for a particular building and yields a guide range of parameters for further use in the subsequent Indoor Aerosol Model (IAM) approach.

With the quantified P, λ, and ($\lambda + \lambda_d$), E can thus be solved based on Equation (1). In some studies, for example, Wallace et al[46] and Isaxon et al,[47] this approach was further simplified assuming that E dominates the left side of the Equation (1) while indoor sources are active:

$$\frac{E}{V} \cong \frac{dI}{dt} \quad (4)$$

To facilitate comparison of these two methods under this approach, emission rates are defined as $E_{\text{SPA+}}$ and E_{SPA} for including and excluding dynamic processes [P, λ, and ($\lambda + \lambda_d$)], respectively.

In this paper, the detection limit for a "source" is $\bar{I}_t + 2 \times sd_t$, where $\bar{I}_t$ is the mean indoor PNC during one hour from time t, and sd_t is the standard deviation of the corresponding period. Statistical analysis was carried out using RStudio (R version 3.3.2, Package *stats* version 3.3.2).

2.2.2 | Indoor Aerosol Model approach (IAM)

The estimates of the particle emission rates and the building penetration factor are expected to be more accurate when all terms in Equation (1) are considered. In this work, we use the single-compartment form of the indoor aerosol model (IAM) developed by Hussein et al,[15,44] incorporating ventilation, particle infiltration, and penetration from outdoors, as well as deposition and coagulation indoors. This approach combines IAM simulations with experimental time series of indoor and outdoor aerosol parameters, which proved to be an effective method to estimate particle number.[15]

The model uses the measured outdoor PNC and geometric mean diameter (GMD) of the experimental indoor PNSD as a time-dependent input. Indoor GMD is the essential parameter that controls particle size-dependent aerosol dynamics. From this, the model computes the time-dependent particle deposition coefficient λ_d, and the coagulation coefficient K ($cm^3\ s^{-1}$). The ventilation rate λ, and

TABLE 2 Summary of main activities

Main activities	*n*	Mean duration[a] (min)	Mean GMD (nm)	Mean PNC (cm^{-3})
Open window	339	38	34	9361
Bake	81	40	30	60 758
Fry	91	25	33	34 188
Toast	56	33	25	19 623
Other cooking	117	36	31	12 805
Candle	92	33	20	109 729
Fireplace	27	30	41	23 702
Vacuum cleaning	28	27	26	11 437
Mixed	78	42	27	31 821
Others	33	25	34	10 447
Unknown	208	26	29	26 559

Note: GMD describes the mean geometric mean diameter of the PNSD observed at event peak time.

Abbreviation: PNC, particle number concentration.

[a]The duration here is the time from the beginning of each source event to the time when indoor PNC reaches maximum.

the building shell penetration factor *P* serve as additional input parameters that are optimized in an interactive process. Our approach retains the information on the evolution of the PNSD, while representing a concession to reduce the complexity of numerical procedures and computation times.

In this version of IAM, the particle deposition rate λ_d was computed as:

$$\lambda_d = \sum_i \frac{A_i}{V} v_{d,i} \quad (5)$$

where $v_{d,i}$ (m s^{-1}) are the deposition velocities of aerosol particles onto the various indoor surfaces (ie, floor, ceiling, and walls) with an area A_i. The surface/volume ratio (A/V) of our 40 homes are listed in Table 1. The $v_{d,i}$ was computed by using the model developed by Lai, Nazaroff[61] the estimated friction velocity (u) near indoor surfaces, and the experimental indoor GMD as input variables.

For coagulation, we consider Brownian diffusion as the dominating process for submicrometer particles. The coagulation rate *K* was calculated based on Fuchs's theory[62] in the transition and free molecular regime.[63] In our quasi-monodisperse formulation *K* is a direct function of GMD (see Figure S1 in the Supporting Information), the coagulation rate between two particles being

$$J_{\text{coagulation}} = KI^2 \quad (6)$$

2.2.3 | Interactive tuning with IAM

For the IAM simulations, the air exchange rate λ and the penetration factor P were tuned so that simulated and experimental indoor PNC (I_{exp} and I_{sim}, respectively) were brought to an agreement. The tuning was performed manually, and interactively on a grid as fine as 5 min time resolution, starting with the estimates of λ and *P* obtained by the SPA approach described in Section 2.2.1.

With optimum values of λ, *P*, λ_d, and K, I_{exp} and I_{sim} were matched for those periods without an apparent influence of indoor sources. During periods of indoor source events, λ and *P* were assumed to be the same as before the event; deviations between I_{exp} and I_{sim} were attributed to the source emissions as follows:

$$\frac{d(I_{\text{exp}} - I_{\text{sim}})}{dt} = P\lambda O - (\lambda + \lambda_d)(I_{\text{exp}} - I_{\text{sim}}) - K(I_{\text{exp}}^2 - I_{\text{sim}}^2) + \frac{E_{\text{IAM}}}{V} \quad (7)$$

The emission rate (E_{IAM}) was then determined from Equation (7). In some cases, λ and *P* needed to be tuned again after a source event, so that the decay pattern of I_{sim} would match that of I_{exp}.

3 | MODEL SIMULATION AND SOURCE-SPECIFIC EMISSION RATES

3.1 | Classification of residential indoor source activities

During the two-year measurement program, more than 1100 activities by residents were identified. Around 900 of these could be classified according to the residents' activity log (see Table 2). The most frequent single activities included opening the window(s), baking, frying, toasting, other cooking (eg, boiling, heating up food, stewing), candle burning, use of a fireplace, vacuum cleaning. In real-life conditions, inhabitants often perform several activities at the same time, such as opening the window while cooking. Such cases are categorized as "mixed" activities. Some activities were seldom recorded, for example, children playing, ironing, doing the laundry, mopping and were summarized among "others." Significant peaks in the indoor

PNC time series that had no corresponding entry in the activity log were categorized as "unknown."

In/around the time of the activities we have classified, peaks can be observed in the time series of indoor PNC. However, there are about five examples from "other cooking," where no noticeable increase in PNC was observed. Our hypothesis is that these "cooking" events were not particle sources, for example, boiling water on a clean stove. Since they did not contribute to indoor PNC, these events are not included in our analysis of particle number emission rates.

In most cases, the increase in indoor PNC stopped as soon as the indoor source had stopped, so the peak time (ie, when the indoor PNC reaches the maximum value) was also when the activity ended. However, for many fireplace (wood stove) activities, there was only one distinct peak in the time series of indoor PNC at the beginning of each activity (see Figure S2 in the Supporting Information). This indicates there was particle emission during flame ignition. Once the door of the stove was closed, the chimney usually worked well enough to conduct smoke particles outside. Since our focus is on the contribution to indoor particle exposure, peak time is treated as the source end time in such cases.

The type and duration of indoor activities varied greatly between the households. The total duration of indoor activities varied from less than 5 min day^{-1} to almost 6 h day^{-1} (see Figure 1). The average duration of activities, excluding opening windows, was 60 ± 40 min day^{-1} in each home. Opening windows and cooking-related activities were the most often occurring activities at home (31% and 30% of total activity duration, respectively). Most of the "open windows" activities took place in the morning, with the peak time around 07:00. The indoor sources frequently occurred at around 08:00, 12:00, and 18:00, which are typical times for breakfast, lunch, and dinner (see Figure S3 in the Supporting Information).

Figure 2 shows the mean PNSD increment caused by single indoor sources and opening windows – determined by subtracting the PNSD at activity start time from the PNSD at peak time. The highest particle number contribution of baking, frying, toasting, cooking, and using a fireplace was to the particles in 20–50 nm size range. Candle burning contributed particles mainly in the 10–20 nm diameter range. By opening windows, indoor PNC increased as well due to the infiltration of outdoor particles, but the corresponding contribution to PNC was much lower compared with indoor sources. The mean PNC during each indoor source are listed in Table 2. The PNSD associated with each source activity showed a broad particle mode, whose mean GMD of each activity is summarized in Table 2.

3.2 | Setting the environment and preparing input for model simulations

With the aid of the SPA approach, a basic set of simulation parameters was derived for each of the households under study. The mean ventilation rate for the 40 different residences was 0.2 ± 0.2 h^{-1} and 3.7 ± 2.8 h^{-1} with closed and opened windows (at least one window is opened), respectively.[51] The mean penetration factor for PNC was 0.6 ± 0.2 cm^{-3}. These two parameters were used as a starting point for the tuning process to achieve the best agreement between simulated indoor PNC (I_{sim}) and measured indoor PNC (I_{exp}).

The mean particle decay rate ($\lambda + \lambda_d$) for PNC calculated using the SPA approach based on Equation (3) was 0.7 ± 0.3 h^{-1}. Figure 3 shows the size-resolved decay rate during each hour after the peak time of an indoor source event. The decay is most pronounced in the ultrafine particle size range, where the losses owing to coagulation and diffusion are the most relevant. Former studies[64,65] concluded that particle coagulation is negligible for indoor PNC below 10^4 cm^{-3}. To avoid a major bias from coagulation, the periods to analyze PNC decay rates were limited to indoor PNC ≤ 10^4 cm^{-3}. The size-resolved particle decay rates served as the references for retrieving the best-fit friction velocity u (m s^{-1}) by using the model developed by Lai, Nazaroff[61] (eg, see Figure 4). The best-fit friction velocity in the 40 homes varied between 0.02 and 0.20 m s^{-1} (see Table 1). Time-resolved particle deposition rates (λ_d) can, therefore, be calculated based on Equation (5).

When deriving a suitable friction velocity, we assumed that the surface of the floor and the ceiling act morphologically in the same way. Differences in furniture, movable and immovable items, could

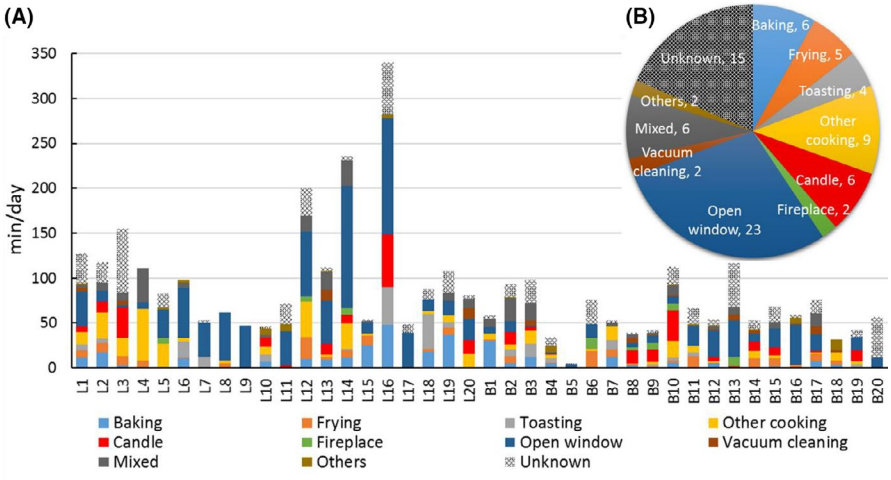

FIGURE 1 (A) Mean duration of indoor source activities identified per day in each home (min/day) and (B) aggregate mean durations (min/day) for the entire dataset (500 days)

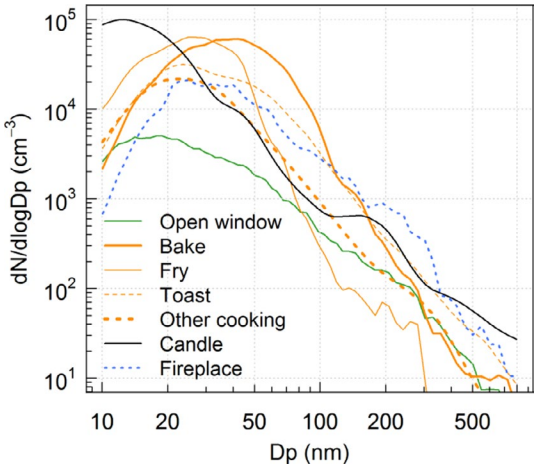

FIGURE 2 Mean PNSD increment resulting from indoor source events. The effect of opening the window (leading to the infiltration of outdoor aerosol) is added for comparison. Dp: particle diameter in nm

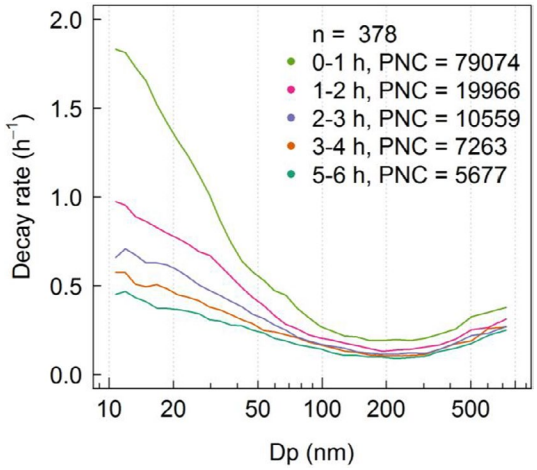

FIGURE 3 Median particle decay rates during each hour after "peak time" of 378 indoor source events. PNC indicates the mean indoor PNC during each hour. This figure includes only activities after which no other activity took place for at least six hours

not be considered explicitly because of their great variations across the 40 dwellings. A sensitivity analysis of the possible effects of surface area changes due to furnishing suggests a negligible influence on λ_d (See Section 3.2 in the Supporting Information).

Based on the experimental indoor GMD, IAM yielded coagulation coefficients on the order of 10^{-6} cm^3 h^{-1}. Observations of indoor PNC could easily exceed 10^4 cm^{-3} during indoor source activity and, since the $J_{coagulation}$ is a function of I^2 the particle losses due to coagulation thus strongly depended on indoor PNC (see Figure S4 in the Supporting Information).

Comparing the dynamic parameters calculated from both approaches, the mean values of $(\lambda + \lambda_d)$ and P show a good agreement (see Table 3). The discrepancy of the mean λ from two approaches could be a result of limitations of the CO_2 decay method, particularly when the inhabitants' activity was not constant. Moreover, λ likely varies with meteorological conditions, and the indoor air turbulences induced by the motion of inhabitants.

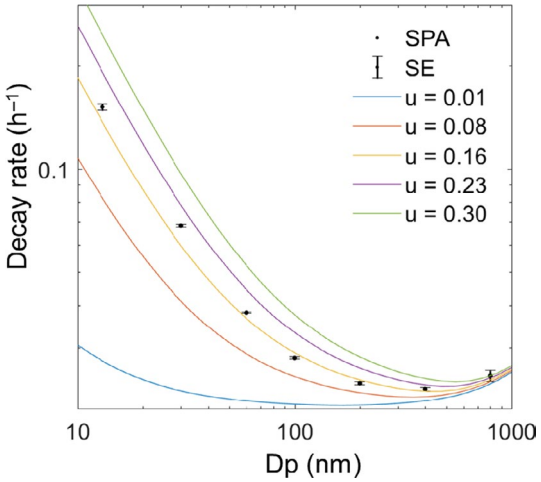

FIGURE 4 Comparison of experimental-derived particle decay rates (dots, SE the standard error) and model predicted decay rates (lines) including deposition onto indoor surfaces for various friction velocities according to Lai, Nazaroff,[61] and Hussein et al[69] Input parameter: $\lambda = 0.2$ h^{-1}, and the indoor surface-area-to-volume ratio (A/V) for the present room 1.7 m^{-1}. The best-fit result for the friction velocity u was 0.16 m s^{-1}

TABLE 3 Mean and standard deviation (SD) of dynamic parameters estimated via single-parameter approach (SPA) and indoor air model approach (IAM)

	SPA approach		IAM approach[a]	
	Mean	SD	Mean	SD
Ventilation rate λ (h^{-1}) (window closed)	0.2	0.2	0.4	0.2
Ventilation rate λ (h^{-1}) (window open)	3.7	2.8	1.6	1.2
Deposition rate λ_d (h^{-1})	–	–	0.2	0.1
Decay rate $(\lambda + \lambda_d)$ (h^{-1})	0.7	0.3	0.7	0.7
Penetration factor P	0.6	0.2	0.6	0.2
Coagulation coefficient K (cm^3 h^{-1})	–	–	7.8×10^{-6}	6.0×10^{-7}

[a] λ and P tuned to match simulated and experimental indoor PNC.

3.3 | IAM model simulations

Figure 5 shows an exemplary simulation of indoor PNC with IAM during one week in home L2. As can be seen, the simulation is able to reproduce indoor PNC with good agreement compared to the

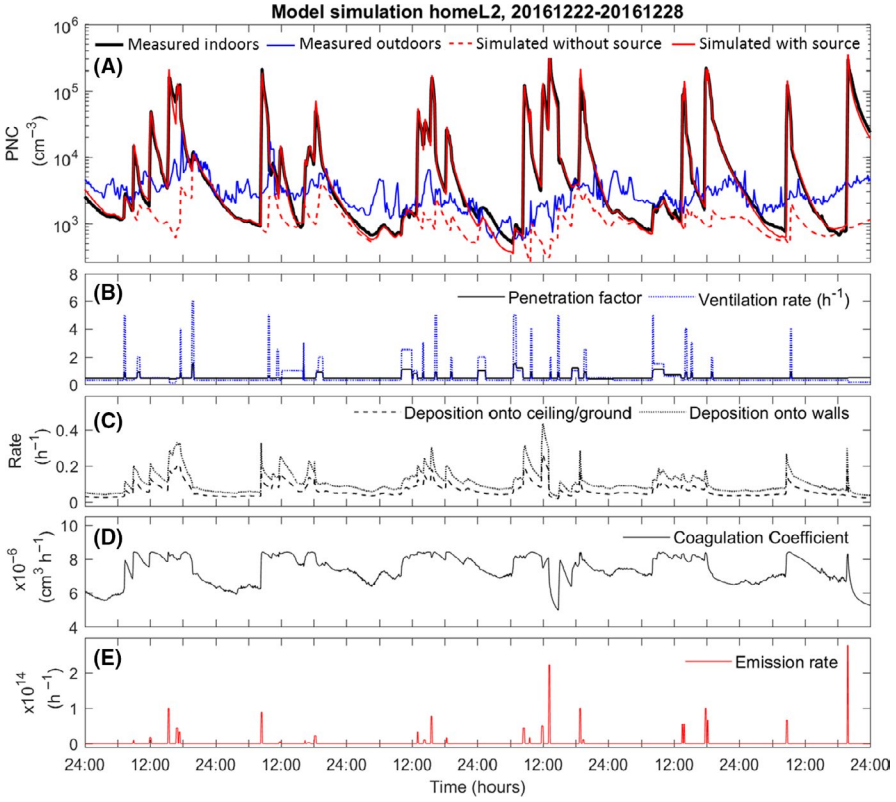

FIGURE 5 Exemplary model simulation of PNC with IAM in one home (No. L2). The model uses measured outdoor PNC and indoor GMD to simulate indoor particle deposition loss, coagulation loss, and indoor PNC. Emission rates are calculated from the difference between simulated and measured indoor PNC

TABLE 4 Comparison of particle number emission rates estimated from the single-parameter approach excluding and including dynamic parameters (E_{SPA} and E_{SPA+}, respectively), as well as the indoor aerosol model approach (E_{IAM})

	Emission rate × 10^{13} (h^{-1})			Correction factors for E_{SPA}		
	E_{SPA}	E_{SPA+}	E_{IAM}			
	Mean ± SD	Mean ± SD	Mean ± SD	$P\lambda O$	$(\lambda + \lambda_d)$	K
Bake	1.5 ± 2.4	2.0 ± 2.8	4.0 ± 6.2	2029	0.8	7.6×10^{-6}
Fry	1.8 ± 2.6	2.2 ± 3.8	3.0 ± 4.8	6407	0.9	7.7×10^{-6}
Toast	2.7 ± 6.1	2.9 ± 6.6	4.7 ± 11.1	2303	0.7	7.6×10^{-6}
Other cooking	0.6 ± 1.0	0.7 ± 1.2	1.5 ± 3.6	–	–	–
Candle	1.9 ± 3.8	2.9 ± 4.1	5.3 ± 6.8	1995	0.8	8.8×10^{-6}
Fireplace	0.8 ± 0.9	0.9 ± 0.9	1.4 ± 1.9	–	–	–
Vacuum cleaning	0.2 ± 0.4	0.3 ± 0.4	0.5 ± 0.7	–	–	–
Mixed	2.1 ± 5.4	2.3 ± 6.1	4.2 ± 8.7	–	–	–
Others	0.3 ± 0.5	0.3 ± 0.5	0.6 ± 1.7	–	–	–
Unknown	0.9 ± 2.9	1.1 ± 3.0	1.5 ± 4.0	–	–	–

Note: Correction factors are offered to adjust E_{SPA} based on formula: $E_{SPA}-P\lambda O+(\lambda + \lambda_d)I + KI^2$.

measured indoor PNC (I_{sim}/I_{exp} = 1.02; R^2 = 0.92). The penetration factor and ventilation rate were $0.4 < P < 1.5$ and $0.1 < \lambda < 6$ h^{-1}, depending on the particular moment of time (see Figure 5B). The sudden increases in P and λ were associated with the inhabitants opening the windows. Changes in λ only—presumably caused by residents' movement, could also be identified and considered in the simulation.

The calculated total deposition rates onto surfaces and coagulation coefficients were 0.1–1 h^{-1} and 5×10^{-6}–8×10^{-6} cm^3 h^{-1}, respectively (see Figure 5C,D). Both parameters were computed from measured indoor GMD; therefore, their variation in the time series follows the evolution of the PNSD, which varies particularly strongly during indoor source events.

3.4 | Indoor sources' emission rate

The observed indoor source events were usually short and intense. We assume, therefore, the emission rate to be constant during the emission period. The mean emission rate estimated via the modal approach (E_{IAM}) of all the indoor sources in 500 days' measurements was 2.7×10^{13} ($\pm 5.9 \times 10^{13}$) h^{-1}. The emission rate shows great overall

variations, even within the same home (see Figure 5E), it varied by two orders of magnitude (from 1.5×10^{12} h^{-1} to 2.0×10^{14} h^{-1}).

During the entire measurement periods, the emission rates of all sources varied between 1×10^{10} h^{-1} and 6×10^{14} h^{-1}, while the mean emission rate of each source type was typically on the order of 10^{13} h^{-1} (see the result of E_{IAM} in Table 4 and Figure 6C). The highest emission rate was obtained for burning candles with mean E_{IAM} of 5.3×10^{13} h^{-1}. The emission rate of using fireplaces, however, was only a quarter of that, although both are combustion sources. Another combustion source is using incense sticks (classified under "Others"), but only one case was reported and the emission rate was 2×10^{12} h^{-1}.

Generally, our results of E_{IAM} are in broad agreement with results from chamber and test room studies. Buonanno et al[35] determined emission rates for frying on an electric stove at different temperatures and with different types of food, the result varied between 1.7×10^{13} h^{-1} and 7.8×10^{13} h^{-1}. Torkmahalleh et al[34] estimated the emission rate of frying with different oils for 2.0×10^{13} h^{-1}–2.1×10^{14} h^{-1}. Schripp et al[29] determined the emission rate of the toaster and electric oven for 1.6×10^{14} h^{-1} and 6.6×10^{13} h^{-1}, respectively. Different types of candles were tested in the studies from Stabile et al[30] and Klosterköther et al,[32] and the particle emission rates varied from 3.0×10^{14} h^{-1} to 6.9×10^{14} h^{-1}.

For studies in real-world conditions, results are shown in Figure 6 in the sub-graph of the corresponding calculation approach. The emission rate calculated by Wallace and Ott[46] and He et al[43] shows good agreement with this study in general. Note that in Wallace and Ott,[46] the electric stove cooking was not separated between frying and boiling and is marked in the "Other cooking" category in Figure 6A. Results of Isaxon et al,[47] however, are all significantly higher than of this study and Wallace and Ott.[46] In their discussion of the limitation, the authors mentioned the accuracy of the instruments used and the possible overestimation of PNC measured by the Nanotracer. In studies of Hussein et al,[42,44] the aerosol dynamics model approach was applied to estimate emission rate in one home in Finland and Prague, respectively. In both homes, the strongest particle number source was cooking, with emission rate for 3.4×10^{13} h^{-1} and 3.6×10^{13} h^{-1} in Finland and Prague, respectively.

The processes that influence the particle emission rates of indoor sources have not yet been fully investigated. Former studies found BTEX from the incomplete combustion of the candle, which are typical precursors of the particulate matter.[18] Klosterköther et al[32] observed different profiles of particle number emission rate and particle size during ignition, normal burning, and extinction phases of burning candle activity. For a wood-burning fireplace, the formation of particulate matter and other pollutants depends on the type of fuel the flame conditions.[20,66] Wallace et al[33] observed the emission of the ultrafine particle from heated empty cooking pans, where the authors stated the desorption/nucleation of sorbed organic matter as the primary source.

We need to acknowledge that for the homes where the kitchen and living room are separated by doors (see Table S1 in

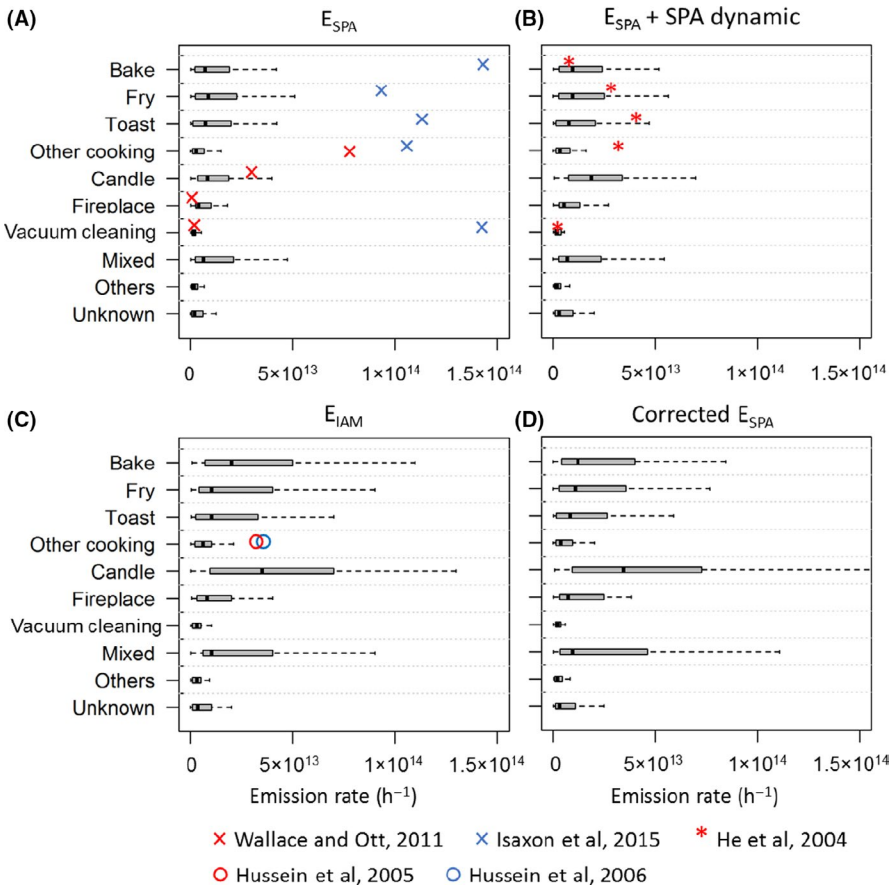

FIGURE 6 Emission rates of each indoor activity estimated by (A) single-parameter approach (SPA), (B) SPA including P, λ, and $(\lambda + \lambda_d)$, (C) indoor air model approach, and (D) SPA with correction. Box plots show the median, 25th, and 75th percentile, and the whiskers are 5th and 95th percentile. The mean emission rates calculated by Wallace and Ott,[46] Isaxon et al,[47] He et al,[43] Hussein et al[42,70] are compared in the plot using the same approach

Supporting Information), our emission rates might underestimate the real cooking-related emission rate. For cooking-related activities, E_{IAM} in homes with separated kitchen is lower compared with open kitchen (see Table S2 in the Supporting Information). We expect the emission rates obtained for the open kitchen/living room combination to be more realistic, acknowledging the non-adequacy of the single-compartment model for the case of a separate kitchen.

Another fact that caught our attention is that most of the investigated houses are equipped with a range hood (see Table S1 in the Supporting Information). However, during the measurement, they were rarely used by the residents. Overall, the range hood was turned on during 38 out of 130 cooking-related activities (ie, baking, roasting, and other cooking; toasting was not involved because people never used the hood during toasting) in 15 homes. When comparing the emission rates of these activities, no clear trend of the effect of using range hoods could be observed (see Figure S5 in the Supporting Information). One reason for this could be that the number of cases is not sufficient to capture the effects. Another reason could be that compared with the effect of the range hood, the emission rates of indoor sources are more sensitive to the cooking habits and preferences of the inhabitants, for example, the ingredients used, the stove temperature.

3.5 | Correction factor for the simplified single-parameter approach

We now introduce a possibility to make emission rates derived from different levels of analysis of the experimental data mutually comparable. As can be seen in Table 4 and Figure 6A–C, the source emission rates derived from the IAM approach (E_{IAM}) were considerably higher than those obtained from the SPA approach (E_{SPA} and E_{SPA+}). The reduction of E_{SPA+} is rather moderate with a median E_{SPA+} 70% of E_{IAM}. The reason for the underestimation could be the neglect of coagulation losses or the underestimation of particle losses of ventilation and deposition.

While E_{SPA} was quantified with the further simplified method under SPA, that is without considering the aerosol dynamic processes, and the median E_{SPA} is only half as much as E_{IAM}. Since source-specific emission rates are to be considered for exposure assessment, we offer a method to adjust results derived from the simplified SPA approach.

For this purpose, the correction factors should be derived from the aerosol dynamic significance. The larger underestimate of E_{SPA} indicated that the assumption of Equation (4) was only partially valid, that is, $[P\lambda O - (\lambda + \lambda_d)I - J_{coagulation}]$ should have been ≤ 0. E_{IAM} were estimated based on Equation (1); thus, the difference between E_{SPA} and E_{IAM} can be mathematically formulated as:

$$\frac{E_{dif}}{V} = \frac{E_{IAM} - E_{SPA}}{V} = S_{dif} = -P\lambda O + (\lambda + \lambda_d)I + KI^2 \quad (8)$$

Assuming outdoor concentrations remain relatively constant, S_{dif} can be treated as a function of I in quadratic polynomial format (ie $y = a + bx + cx^2$). The mean value of $P\lambda O$, $(\lambda + \lambda_d)$ and K calculated from the IAM approach (3275, 0.9, and 7.7×10^{-6}, respectively) are used as correction factors, which correct the effect of particle penetration from outdoor, indoor deposition loss, and indoor coagulation loss accordingly.

Applying the correction factors as the coefficients in the quadratic polynomial function for known indoor sources, the linear fitted result (S_{fitted}) is illustrated in Figure 7 (formula and line in red color). S_{dif} and S_{fitted} are well correlated in the log scale with $R^2 = 0.7$, p-value «0.05.

Among the known single sources, S_{dif} of baking, frying, toasting, and candle burning all is well correlated with the mean parameter linear fitted result ($R^2 \geq 0.7$, p-value «0.05, see Figure S6 in the Supporting Information). These sources function as a relatively constant source of particle number emissions, that is, with less influence from the operating habits of residents. For these sources, correction factors are recommended when calculating the E_{SPA} (see Table 4). For other cooking, vacuum cleaning, and using fireplaces, however, due to the inconstant emission, the R^2 is much lower (0.6, 0.6, and 0.2, respectively). The extremely low correlation in the use of fireplaces could be attributable to the emissions being highly dependent on the way residents start fires.

The corrected results of each indoor source all show good agreement with E_{IAM} (see Figure 6D) with the median of corrected E_{SPA} 93% of E_{IAM}. For future measurements where only indoor PNC is available, the mean parameters could be used as the correction

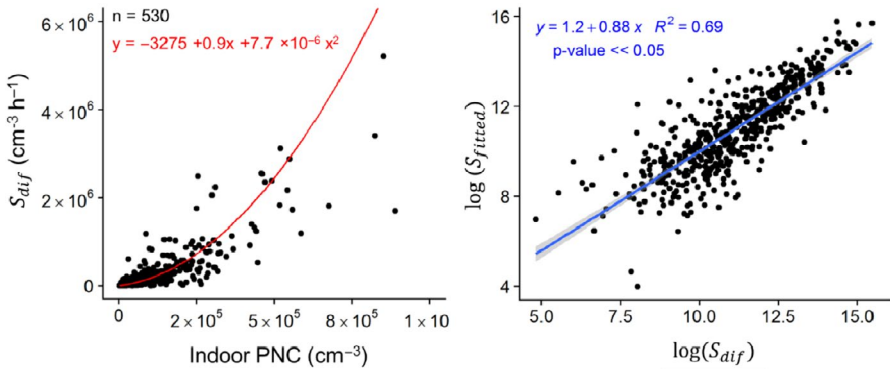

FIGURE 7 S_{dif} and mean parameter fitting as a function of indoor PNC (left); Scatter plot of log(S_{dif}) and log(S_{fitted}) (right). Number of events $n = 530$

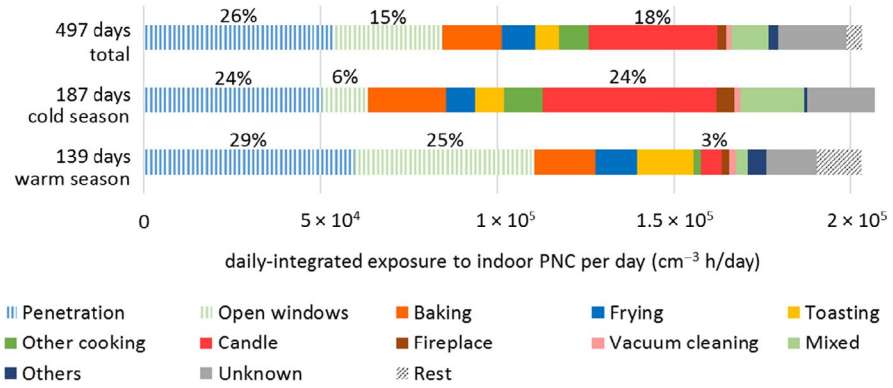

FIGURE 8 Mean source contribution to daily-integrated exposure to indoor PNC per day (cm^{-3} h day^{-1}). Data of this figure are available in Table S3 in the Supporting Information

factors for the rapid estimation of emission rates. This is also a feasible approach for residents to better understand the level of indoor emission in their daily lives. This estimation is more suitable for homes with similar conditions, for example, relatively airtight, naturally ventilated, and under rather low ventilation conditions.

With respect to the limitations of our approach, one needs to keep in mind that all calculations are based on the well-mixed single-compartment model approach applied for different configurations of homes. There might be internal air exchanges in indoor spaces that have influenced the estimated parameters and could, therefore, lead to an underestimation of the particle emission rates.

4 | SOURCE CONTRIBUTION FROM INDOOR AND OUTDOOR

Having simulated indoor time series of PNC for the 40 dwellings using the IAM model, we are now able to differentiate the fractions of indoor PNC that originate from indoor and outdoor sources, respectively. Distinguishing these particle types might represent a key for a better understanding of indoor particle exposure.[67] According to previous works,[16] indoor exposure to submicrometer particles emitted from indoor and outdoor sources can be quantified as a daily-integrated exposure, which was calculated by integrating the PNC over time and dividing by the number of measurement days (cm^{-3} h day^{-1}).

The daily-integrated exposure in our 40 households varied from 0.7×10^5 to 4.7×10^5 cm^{-3} h day^{-1} (see Figure S7 in the Supporting Information), with a total mean around 2×10^5 cm^{-3} h day^{-1} (see Figure 8). Indoor sources contributed 56% of total indoor particle number exposure, with burning candles contributing the biggest individual amount. The contribution from outdoor aerosols was calculated from the IAM simulation of indoor PNC disregarding indoor source events, resulting in a relative share of 42% in total exposure. The IAM model approach even allows us to break this contribution down to penetration through the building shell, and ventilation through windows (26% and 15%, respectively). The remaining gap in the balance (ie, "Rest" in Figure 8) amounting to approximately 2% of total exposure could stem from resuspension or unidentified minor sources.

Although indoor source events proved to be rather short-lived, their significant contribution to indoor PNC exposure derives from their high source emission rates and the rather moderate decay rate, which leads to residence times of several hours for particles emitted indoors if not vented.

The daily exposure burden was similar in the cold and warm seasons – around 2×10^5 cm^{-3} h day^{-1} (see Figure 8). However, due to the different behavior patterns of residents in the cold and warm seasons, the proportions of indoor and outdoor contributions were rather different. In the cold season, residents were exposed to a majority of particles emitted from indoor sources (70%) whereas, in the warm season, the corresponding identified contribution amounted to only 39% of total exposure. Opening windows and burning candles were the two major activities that made the crucial difference (their proportions of total exposure were 6% and 24% in the cold season, 25% and 3% in the warm season, respectively). Without burning candles, the daily indoor exposure would have been reduced by approximately 5×10^4 cm^{-3} h day^{-1} in the cold period.

Compared with previous studies, the daily-integrated exposure burden in our studied German homes is lower. Mullen et al[68] estimated the total contribution from indoor and outdoor sources to the daily-integrated exposure in two homes in Beijing during summer (4–6 days). Compared with the summer season in our study, the contribution of exposure from indoor was similar, while outdoor was twice as high, which could be attributed to the much higher outdoor PNC (mean concentration three times as high). Bhangar et al[16] estimated the daily-integrated exposure in seven homes in California across all four seasons for a total of 26 days. Their contribution of outdoor particles is similar to our study, while the fraction of indoor sources was twice as high. However, as both studies did not analyze the contribution from each specific indoor or outdoor source, it is unclear which indoor source led to the difference.

Bekö et al[27] measured the indoor PNC in 56 Danish homes in the winter period (~45 h each) and estimated the mean daily-integrated exposure for 7×10^5 cm^{-3} h day^{-1}, which is three times as high as in our German homes, and 2 times as high as in residencies both in California and Beijing (see Figure S8 in the Supporting Information). The authors cite the intensive candle burning in Scandinavia as a major influence, the average burning time in observed Danish homes was about 140 min day^{-1}, and in our residences was only

16 min day^{-1} during the winter period. It is evident that our present study offers a significant extension of knowledge related to indoor particle number exposure and source-specific contributions across different seasons.

5 | SUMMARY AND CONCLUSION

In this work, we identified major sources of exposure to submicrometer particles (10–800 nm) and quantified their relative contribution to integrated residential indoor exposure in 40 German homes in over two years. Two methodological approaches (SPA approach; IAM approach) were applied to estimate the particle number emission rates associated with more than 800 indoor source events involving baking, frying, toasting, candle burning, use of fireplaces, and opening windows.

The IAM approach considered particle penetration, ventilation, as well as particle size-dependent coagulation and deposition processes. Matching model simulations and experimental data at high time resolution allowed us to understand and disentangle the effects of the different processes on indoor PNC. The average E_{IAM} of each specific indoor source varied between 0.5×10^{13} h^{-1} (vacuum cleaning) and 5.3×10^{13} h^{-1} (burning candles).

Emission rates calculated from the simplified SPA approach (E_{SPA}) is only half as the emission rate calculated by the model. Correction factors were derived which could make the E_{SPA} better comparable. For houses under similar conditions, the correction factors can be applied to correct the previous results of E_{SPA} and estimate emission rates using only indoor PNC data. In general, to estimate a high-quality emission rate, it is crucial to quantify the main aerosol dynamic processes that influence changes in indoor PNC.

Budget calculations yield that indoor sources are the major contributors (~56%) to the mean PNC exposure in our 40 homes. Outdoor sources contributed ~ 42% of total PNC exposure, which could be differentiated between building shell penetration (~26%) and infiltration through open windows (~15%). During the cold period, the contribution from indoor sources even took up to 70% of the exposure due to the increasing use of candles. Reducing the uses of candles, especially in modern homes with low penetration and low ventilation rates is a prime measure to reduce overall indoor PNC exposure. The daily-integrated exposure in our 40 homes is lower than the values reported from other countries (California, Beijing, and Copenhagen). The reasons are resulting from the lower outdoor PNC and less contributions from indoor emissions.

To the best of our knowledge, this dataset is one of the largest, which includes source-specific emission rates and particle exposure in residential environments. This study fills the gap of knowledge of the emission rate in European houses and provides a better understanding of emission rates calculated via two different approaches. Our results suggest that indoor sources are still responsible for the majority of number-related residential exposure to submicron particles, which should be taken into consideration in epidemiological studies and risk assessment when investigating the effects of aerosol particles on health.

ACKNOWLEDGMENTS

This work was supported by the Federal Ministry for the Environment, Nature Conservation, Building and Nuclear Safety (BMUB) grant UFOPLAN FKZ 3715 61 200 (German title: „*Ultrafeine Partikel im Innenraum und in der Umgebungsluft: Zusammensetzung, Quellen und Minderungsmöglichkeiten*"), initiated by Anja Daniels (UBA). We thank the 40 volunteering families, providing access to their homes for our measurements and log their activities. We thank the assistants of TROPOS, notably Thomas Lettau, Tanzina Akther, for their helpful assistance in data analyses.

CONFLICT OF INTEREST

The authors declare no conflict of interest.

AUTHOR CONTRIBUTIONS

Jiangyue Zhao: Conceptualization (equal); Data curation (lead); Formal analysis (lead); Methodology (supporting); Validation (lead); Visualization (lead); Writing—original draft (lead); Writing—review and editing (equal). **Wolfram Birmili**: Funding acquisition (lead); Project administration (equal); Writing—review and editing (equal). **Tareq Hussein**: Conceptualization (equal); Methodology (lead); Writing—review and editing (equal). **Birgit Wehner**: Project administration (supporting); Supervision (supporting); Writing—review and editing (equal). **Alfred Wiedensohler**: Resources (lead); Project administration (equal); Supervision (lead); Writing—review and editing (equal).

PEER REVIEW

The peer review history for this article is available at https://publons.com/publon/10.1111/ina.12773.

DATA AVAILABILITY STATEMENT

Data available on request from the authors.

ORCID

Jiangyue Zhao https://orcid.org/0000-0001-5202-239X
Wolfram Birmili https://orcid.org/0000-0002-5295-6333

REFERENCES

1. Pope CA III, Dockery DW. Health effects of fine particulate air pollution: lines that connect. *J Air Waste Manag Assoc*. 2006;56(6):709-742.
2. Brook RD, Rajagopalan S, Pope CA, et al. Particulate matter air pollution and cardiovascular disease: an update to the scientific statement from the American Heart Association. *Circulation*. 2010;121(21):2331-2378.
3. Donaldson K, MacNee W. Potential mechanisms of adverse pulmonary and cardiovascular effects of particulate air pollution (PM10). *Int J Hyg Environ Health*. 2001;203(5–6):411-415.
4. Fitzmaurice C, Akinyemiju TF, Al Lami FH, et al. Global, regional, and national cancer incidence, mortality, years of life lost, years lived with disability, and disability-adjusted life-years for 29 cancer

groups, 1990 to 2016: a systematic analysis for the global burden of disease study. *JAMA Oncol*. 2018;4(11):1553-1568.
5. Chen G, Li S, Zhang Y, et al. Effects of ambient PM1 air pollution on daily emergency hospital visits in China: an epidemiological study. *Lancet Planet Health*. 2017;1(6):e221-e229.
6. Akther T, Ahmed M, Shohel M, Ferdousi F, Salam A. Particulate matters and gaseous pollutants in indoor environment and Association of ultra-fine particulate matters (PM1) with lung function. *Environ Sci Pollut Res*. 2019;26(6):5475–5484.
7. Cohen AJ, Brauer M, Burnett R, et al. Estimates and 25-year trends of the global burden of disease attributable to ambient air pollution: an analysis of data from the Global Burden of Diseases Study 2015. *Lancet*. 2017;389(10082):1907-1918.
8. Brasche S, Bischof W. Daily time spent indoors in German homes – Baseline data for the assessment of indoor exposure of German occupants. *Int J Hyg Environ Health*. 2005;208(4):247-253.
9. Leech JA, Nelson WC, Burnett RT, Aaron S, Raizenne ME. It's about time: a comparison of Canadian and American time–activity patterns. *J Expo Sci Environ Epidemiol*. 2002;12(6):427-432.
10. Morawska L, Ayoko GA, Bae GN, et al. Airborne particles in indoor environment of homes, schools, offices and aged care facilities: The main routes of exposure. *Environ Int*. 2017;108:75-83.
11. Morawska L, Afshari A, Bae GN, et al. Indoor aerosols: from personal exposure to risk assessment. *Indoor Air*. 2013;23(6):462-487.
12. Mazaheri M, Lin W, Clifford S, et al. Characteristics of school children's personal exposure to ultrafine particles in Heshan, Pearl River Delta, China–a pilot study. *Environ Int*. 2019;132:105134.
13. van Nunen E, Vermeulen R, Tsai M-Y, et al. Associations between modeled residential outdoor and measured personal exposure to ultrafine particles in four European study areas. *Atmos Environ*. 2020;226:117353.
14. García-Hernández C, Ferrero A, Estarlich M, Ballester F. Exposure to ultrafine particles in children until 18 years of age: a systematic review. *Indoor Air*. 2020;30(1):7-23.
15. Bhangar S, Mullen N, Hering S, Kreisberg N, Nazaroff W. Ultrafine particle concentrations and exposures in seven residences in northern California. *Indoor Air*. 2011;21(2):132-144.
16. Wallace L, Jeong SG, Rim D. Dynamic behavior of indoor ultrafine particles (2.3-64 nm) due to burning candles in a residence. *Indoor Air*. 2019;29(6):1018-1027.
17. Derudi M, Gelosa S, Sliepcevich A, et al. Emission of air pollutants from burning candles with different composition in indoor environments. *Environ Sci Pollut Res*. 2014;21(6):4320-4330.
18. Hussein T, Wierzbicka A, Löndahl J, Lazaridis M, Hänninen O. Indoor aerosol modeling for assessment of exposure and respiratory tract deposited dose. *Atmos Environ*. 2015;106:402-411.
19. Manigrasso M, Vitali M, Protano C, Avino P. Temporal evolution of ultrafine particles and of alveolar deposited surface area from main indoor combustion and non-combustion sources in a model room. *Sci Total Environ*. 2017;598:1015-1026.
20. Salthammer T, Schripp T, Wientzek S, Wensing M. Impact of operating wood-burning fireplace ovens on indoor air quality. *Chemosphere*. 2014;103:205-211.
21. Azimi P, Zhao D, Pouzet C, Crain NE, Stephens B. Emissions of ultrafine particles and volatile organic compounds from commercially available desktop three-dimensional printers with multiple filaments. *Environ Sci Technol*. 2016;50(3):1260-1268.
22. Lamorena RB, Lee W. Influence of ozone concentration and temperature on ultra-fine particle and gaseous volatile organic compound formations generated during the ozone-initiated reactions with emitted terpenes from a car air freshener. *J Hazard Mater*. 2008;158(2–3):471-477.
23. Rohr AC, Weschler CJ, Koutrakis P, Spengler JD. Generation and quantification of ultrafine particles through terpene/ozone reaction in a chamber setting. *AS&T*. 2003;37(1):65-78.
24. Langer S, Ramalho O, Derbez M, Ribéron J, Kirchner S, Mandin C. Indoor environmental quality in French dwellings and building characteristics. *Atmos Environ*. 2016;128:82-91.
25. Wallace L. Indoor sources of ultrafine and accumulation mode particles: size distributions, size-resolved concentrations, and source strengths. *Aerosol Sci Technol*. 2006;40(5):348-360.
26. Diapouli E, Eleftheriadis K, Karanasiou AA, et al. Indoor and outdoor particle number and mass concentrations in Athens. sources, sinks and variability of aerosol parameters. *Aerosol Air Qual Res*. 2011;11(6):632–642.
27. Bekö G, Weschler CJ, Wierzbicka A, et al. Ultrafine particles: exposure and source apportionment in 56 Danish homes. *Environ Sci Technol*. 2013;47(18):10240-10248.
28. Lazaridis M, Eleftheriadis K, Ždímal V, et al. Number concentrations and modal structure of indoor/outdoor fine particles in four European cities. *Aerosol Air Qual Res*. 2017;17(1):131-146.
29. Schripp T, Kirsch I, Salthammer T. Characterization of particle emission from household electrical appliances. *Sci Total Environ*. 2011;409(13):2534-2540.
30. Stabile L, Fuoco F, Buonanno G. Characteristics of particles and black carbon emitted by combustion of incenses, candles and anti-mosquito products. *Build Environ*. 2012;56:184-191.
31. Wallace L, Wang F, Howard-Reed C, Persily A. Contribution of gas and electric stoves to residential ultrafine particle concentrations between 2 and 64 nm: size distributions and emission and coagulation rates. *Environ Sci Technol*. 2008;42(23):8641-8647.
32. Klosterköther A, Kurtenbach R, Wiesen P, Kleffmann J. Determination of the emission indices for NO, NO2, HONO, HCHO, CO, and particles emitted from candles. *Indoor Air*. 2020.
33. Wallace LA, Ott WR, Weschler CJ. Ultrafine particles from electric appliances and cooking pans: experiments suggesting desorption/nucleation of sorbed organics as the primary source. *Indoor Air*. 2015;25(5):536-546.
34. Torkmahalleh MA, Goldasteh I, Zhao Y, et al. PM2. 5 and ultrafine particles emitted during heating of commercial cooking oils. *Indoor Air*. 2012;22(6):483-491.
35. Buonanno G, Morawska L, Stabile L. Particle emission factors during cooking activities. *Atmos Environ*. 2009;43(20):3235-3242.
36. Glytsos T, Ondráček J, Džumbová L, Kopanakis I, Lazaridis M. Characterization of particulate matter concentrations during controlled indoor activities. *Atmos Environ*. 2010;44(12):1539-1549.
37. Knibbs LD, He C, Duchaine C, Morawska L. Vacuum cleaner emissions as a source of indoor exposure to airborne particles and bacteria. *Environ Sci Technol*. 2012;46(1):534-542.
38. Zai S, Zhen H, Jia-song W. Studies on the size distribution, number and mass emission factors of candle particles characterized by modes of burning. *J Aerosol Sci*. 2006;37(11):1484-1496.
39. Géhin E, Ramalho O, Kirchner S. Size distribution and emission rate measurement of fine and ultrafine particle from indoor human activities. *Atmos Environ*. 2008;42(35):8341-8352.
40. Byeon JH, Kim J-W. Particle emission from laser printers with different printing speeds. *Atmos Environ*. 2012;54:272-276.
41. Scungio M, Vitanza T, Stabile L, Buonanno G, Morawska L. Characterization of particle emission from laser printers. *Sci Total Environ*. 2017;586:623-630.
42. Hussein T, Glytsos T, Ondráček J, et al. Particle size characterization and emission rates during indoor activities in a house. *Atmos Environ*. 2006;40(23):4285-4307.
43. He C, Morawska L, Hitchins J, Gilbert D. Contribution from indoor sources to particle number and mass concentrations in residential houses. *Atmos Environ*. 2004;38(21):3405-3415.
44. Hussein T, Korhonen H, Herrmann E, Hämeri K, Lehtinen KE, Kulmala M. Emission rates due to indoor activities: indoor aerosol model development, evaluation, and applications. *Aerosol Sci Technol*. 2005;39(11):1111-1127.

45. Wangchuk T, He C, Knibbs LD, Mazaheri M, Morawska L. A pilot study of traditional indoor biomass cooking and heating in rural Bhutan: gas and particle concentrations and emission rates. *Indoor Air*. 2017;27(1):160-168.
46. Wallace L, Ott W. Personal exposure to ultrafine particles. *J Expo Sci Environ Epidemiol*. 2011;21(1):20-30.
47. Isaxon C, Gudmundsson A, Nordin EZ, et al. Contribution of indoor-generated particles to residential exposure. *Atmos Environ*. 2015;106:458-466.
48. Koivisto AJ, Kling KI, Hänninen O, et al. Source specific exposure and risk assessment for indoor aerosols. *Sci Total Environ*. 2019;668:13-24.
49. Abadie MO, Blondeau P. PANDORA database: a compilation of indoor air pollutant emissions. *HVAC&R Res*. 2011;17(4):602-613.
50. Hussein T. Indoor-to-outdoor relationship of aerosol particles inside a naturally ventilated apartment – a comparison between single-parameter analysis and indoor aerosol model simulation. *Sci Total Environ*. 2017;596–597:321-330.
51. Zhao J, Birmili W, Wehner B, et al. Particle mass concentrations and number size distributions in 40 homes in Germany: indoor-to-outdoor relationships, diurnal and seasonal variation. *Aerosol Air Qual Res*. 2020;20:576-589.
52. Wiedensohler A, Birmili W, Nowak A, et al. Mobility particle size spectrometers: harmonization of technical standards and data structure to facilitate high quality long-term observations of atmospheric particle number size distributions. *Atmos Meas Tech*. 2012;5:657-685.
53. Zhao J, Weinhold K, Merkel M, et al. Concept of high quality simultaneous measurements of the indoor and outdoor aerosol to determine the exposure to fine and ultrafine particles in private homes. *Springer VDI-Verlag, Gefahrstoffe- Reinhal Luft*. 2018;3(3/2018):73-78.
54. Wiedensohler A, Wiesner A, Weinhold K, et al. Mobility particle size spectrometers: calibration procedures and measurement uncertainties. *Aerosol Sci Technol*. 2018;52(2):146-164.
55. Nazaroff WW, Cass GR. Mathematical modeling of indoor aerosol dynamics. *Environ Sci Technol*. 1989;23(2):157-166.
56. Hussein T, Kulmala M. Indoor aerosol modeling: Basic principles and practical applications. *Water Air Soil Pollut Focus*. 2008;8(1):23-34.
57. Jamriska M, Morawska L. Quantitative assessment of the effect of surface deposition and coagulation on the dynamics of submicrometer particles indoors. *Aerosol Sci Technol*. 2003;37(5):425-436.
58. Rim D, Choi J-I, Wallace LA. Size-resolved source emission rates of indoor ultrafine particles considering coagulation. *Environ Sci Technol*. 2016;50(18):10031-10038.
59. Xiao Y, Lv Y, Zhou Y, Liu H, Liu J. Size-resolved surface deposition and coagulation of indoor particles. *Int J Environ Health Res*. 2020;30(3):251-267.
60. Persily AK. Field measurement of ventilation rates. *Indoor Air*. 2016;26(1):97-111.
61. Lai AC, Nazaroff WW. Modeling indoor particle deposition from turbulent flow onto smooth surfaces. *J Aerosol Sci*. 2000;31(4):463-476.
62. Fuchs NA, Daisley R, Fuchs M, Davies C, Straumanis M. The mechanics of aerosols. *PhT*. 1965;18:73.
63. Seinfeld JH, Pandis SN. *Atmospheric Chemistry and Physics: From Air Pollution to Climate Change*, 3 Hoboken, New Jersey: rd ed. John Wiley & Sons; 2016.
64. Hussein T, Hruška A, Dohányosová P, et al. Deposition rates on smooth surfaces and coagulation of aerosol particles inside a test chamber. *Atmos Environ*. 2009;43(4):905-914.
65. Rim D, Green M, Wallace L, Persily A, Choi J-I. Evolution of ultrafine particle size distributions following indoor episodic releases: relative importance of coagulation, deposition and ventilation. *Aerosol Sci Technol*. 2012;46(5):494-503.
66. Lahiri T, Ranjan Ray M.5 Effects of Indoor Air Pollution from Biomass Fuel Use on Women's Health inIndia; *Health and Environmental Impacts* (2010):135-163.
67. Riley WJ, McKone TE, Lai ACK, Nazaroff WW. Indoor particulate matter of outdoor origin: importance of size-dependent removal mechanisms. *Environ Sci Technol*. 2002;36(2):200-207.
68. Mullen NA, Liu C, Zhang Y, Wang S, Nazaroff WW. Ultrafine particle concentrations and exposures in four high-rise Beijing apartments. *Atmos Environ*. 2011;45(40):7574-7582.
69. Hussein T, Smolik J, Kerminen V-M, Kulmala M. Modeling dry deposition of aerosol particles onto rough surfaces. *Aerosol Sci Technol*. 2012;46(1):44-59.
70. Hussein T, Hämeri K, Heikkinen MSA, Kulmala M. Indoor and outdoor particle size characterization at a family house in Espoo-Finland. *Atmos Environ*. 2005;39(20):3697-3709.

SUPPORTING INFORMATION

Additional supporting information may be found online in the Supporting Information section.

How to cite this article: Zhao J, Birmili W, Hussein T, Wehner B, Wiedensohler A. Particle number emission rates of aerosol sources in 40 German households and their contributions to ultrafine and fine particle exposure. *Indoor Air*. 2021;31:818–831. https://doi.org/10.1111/ina.12773